Interaction of folic acid and some MMP inhibitor folate-γ-hydroxamate derivatives with Zn(II) and human serum albumin

Éva A. Enyedy[a*], Etelka Farkas[b], Orsolya Dömötör[a], M. Amélia Santos[c]

[a]Department of Inorganic and Analytical Chemistry, University of Szeged, P.O. Box 440, H-6701 Szeged, Hungary

[b]Department of Inorganic and Analytical Chemistry, University of Debrecen, P.O. Box 21, H-4010 Debrecen, Hungary

[c]Centro de Química Estrutural, Instituto Superior Técnico, 1049-001 Lisboa, Portugal

ABSTRACT

Human serum albumin binding of folic acid and its γ-hydroxamate/carboxylate derivatives was studied by ultrafiltration and spectrofluorimetry, and it was found that the ligands exhibit a moderate binding (K_D ~2-50 μM), and the folate-γ-phenylalanine represents the highest conditional binding constant towards albumin. This feature may have importance in the serum transport processes of these ligands. Interaction of folic acid and its derivatives with Zn(II) was investigated in aqueous solution to obtain the composition and stabilities of the complexes by the means of pH-potentiometry, ^{1}H NMR and electrospray ionization mass spectrometry, together with the characterization of the proton dissociation processes and the hydro-lipophilic properties of the ligands. The formation of *mono*-ligand complexes was demonstrated in all cases and the contribution of the glutamyl carboxylates to the coordination was excluded. Binding of folic acid and its γ-carboxylate derivatives to Zn(II) via the pteridine moiety is suggested, while the (O,O) coordination fashion of the folate-γ-hydroxamate ligands has importance in their inhibitory activity against Zn(II)-containing matrix metalloproteinases. It was found that the enzyme inhibition of these folate-γ-hydroxamate ligands is mainly tuned by other features, such as the lipophilic character rather than the Zn(II)-chelate stability.

Keywords: Solution Equilibrium, Stability Constants, Folic acid, Folate-Hydroxamate Conjugates, Protein-Ligand Interaction, Ultrafiltration

* Corresponding author: Fax: +36 62 420505
E-mail address: enyedy@chem.u-szeged.hu (É.A. Enyedy)

1. Introduction

Folic acid (pteroyl-L-glutamic acid, see Scheme 1) as a vitamin (B_9) is essential for a wide range of biochemical pathways such as nucleotide biosynthesis, therefore, is a key molecule for cell replication. During periods of rapid cell division in various inflammatory states, the majority of malignant cells exceeds the expression of the high affinity folate receptors (FRs), which can selectively facilitate the transport of reduced forms of folic acid via the receptor mediated endocytosis [1-3]. This property makes FR a promising tumor target to deliver folate-linked diagnostic or therapeutic agents [1-3]. *E.g.* several radiolabelled folic acid conjugates such as ^{111}In- diethylenetriaminepentaacetic acid (DTPA)-folate or ^{67}Ga-desferrioxamine-folate were developed for imaging of malignant tissues [4-7].

Scheme 1

Antifolates (methotrexate (MTX), pemetrexed, *etc.*) are also used in the clinical practice of cancer chemotherapy. They can inhibit the enzymes thymidylate synthase and/or dihydrofolate reductase (DHFR) [8,9]. γ-Monohydroxamate derivatives of MTX were synthesized as potential dual target antitumor agents in our former work, and they show inhibitory effect against two independent enzymes involved in metastasizing tumors, DHFR and matrix metalloproteinases (MMPs) [10]. MMPs are zinc-dependent endopeptidases and are frequently overexpressed in tumor progression [11-14]. Hydroxamic acids are particularly potent inhibitors of MMPs due to their bidentate (O,O) coordination to the catalytic Zn(II) center of the enzymes [15,16]. The folic acid analogues of the γ-monohydroxamate-MTX conjugates also represent inhibitory activity against different MMPs (MMP-2, 7, 9, 14) at micromolar level [10]. It was pointed out that insertion of an amino acid spacer (Phe, Pro) between the folate and the hydroxamate moieties improved the inhibitory potency [10]. Moreover, these molecules can be also considered as the model compounds for the MTX-hydroxamate derivatives.

The efficacy of the γ-monohydroxamate-folic acid MMP inhibitor molecules is most likely strongly dependent on their binding ability to the catalytic Zn(II), additionally the fitting to the specificity pocket of the enzyme is also an important issue. On the other hand, the action and bioavailability of a drug can be influenced by other pharmacokinetic parameters such as the potential for binding to human blood serum proteins. It is well known that folic acid and its derivatives following the absorption can appear quickly in the blood circulation. A larger dose of folates may escape metabolism by the liver and they are present in their

original form, but are extensively bound to serum proteins [17]. Among the possible binders the high affinity folate binding protein and α_2-macroglobulin are minor species, while the human serum albumin (HSA) is the most abundant blood serum protein (c_{HSA} = 630 μM) [18-21], thus HSA may have an important role in binding folate conjugates and controlling the concentration the free (available) drug concentration.

Studies on the HSA and Zn(II) binding abilities can provide considerable contribution to the interpretation of the biological activity of the MMP inhibitor folate-hydroxamate conjugates. Therefore, interactions of Zn(II) with folate-γ-hydroxamic acid (Fha), folate-γ-proline hydroxamic acid (FProha) and folate-γ-phenylalanine hydroxamic acid (FPheha), shown in Scheme 1, were studied by different methods in this work. HSA binding strength and sites were also investigated in aqueous solution at physiological pH. Folic acid and the corresponding folate-γ-carboxylic acids (see Scheme 1) were involved for comparison. Moreover, studies on complexation between folic acid and Zn(II) may help to understand the effect of folic acid on Zn(II) homeostasis [22] and only few information is available in the literature about the speciation of Zn(II)-folic acid complexes [23-26].

2. Experimental

2.1. Chemicals

Fha, FProha, folate-γ-proline (FPro), FPheha, folate-γ-phenylalanine (FPhe) were prepared as it was described in our previous paper [10]. Folic acid, acetohydroxamic acid (Aha), benzoylglutamic acid (BzGlu), pterine (Pte), racemic warfarin, human serum albumin (with fatty acids) and apotransferrin (apoTf) were obtained from Sigma-Aldrich. The purity and stability of the folate derivatives, Pte, BzGlu and Aha were checked and the exact concentration of the stock solutions prepared was determined by the Gran method [27]. $ZnCl_2$ stock solution was made by the dissolution of anhydrous $ZnCl_2$ in a known amount of HCl. The Zn(II) concentration was determined by complexometry via the EDTA complex and the accurate HCl concentration in the stock solution was obtained by pH-metric titrations. The concentrations of the protein solutions were estimated from their UV absorption: ε_{280nm}(HSA) = 36850 $M^{-1}cm^{-1}$ and ε_{280nm}(apoTf) = 92300 $M^{-1}cm^{-1}$ [28,29]. 2-(*N*-morpholino)ethanesulfonic acid (MES), 4-(2-hydroxyethyl)-1-piperazineethanesulfonic acid (HEPES), Tris, *N*-cyclohexyl-2-aminoethanesulfonic acid (CHES) buffers and *n*-octanol were

obtained from Sigma-Aldrich. DMSO was freshly distilled before the preparation of the solutions, which were kept in dark.

2.2. pH-Potentiometric studies

The measurements for determining the protonation constants of the ligands and stability constants of the metal complexes were carried out at an ionic strength of 0.10 M (KCl) and at 25.0±0.1 ^{o}C in DMSO:water 60:40 (w/w) mixed solvent as it was found to be sufficient for dissolution of the folate ligands at the concentration level necessary for the pH-metry (*i.e.* ≥1-2 mM). The titrations were performed with a carbonate-free KOH solution of known concentrations (0.10 M). Concentrations of HCl and KOH were determined by pH-potentiometric titrations. An Orion 710A pH meter equipped with Metrohm combined electrode (type 6.0234.100) and Metrohm 665 Dosimat burette were used for the pH-metric measurements. The electrode system was calibrated according to Irving *et al.* [30] and the pH-metric readings could therefore be converted into hydrogen ion concentration. The average water ionization constant, pK_w, is 16.22 ± 0.05 under DMSO:water 60:40 (w/w) solvent mixture condition at 25 ^{o}C [26]. The pH-metric titrations were performed in the pH range of 2.0-13.0. Initial volume of the samples was 5.0 mL. The ligand concentration was in the range 1-2 mM and the metal-to-ligand ratios in the range 1:1-1:4 were used. Due to the low solubility of the ligands, they were added directly to the samples as solids instead of preparing stock solutions. Following the titration of the ligand by KOH, samples were acidified back and the metal stock solution was added. The accepted fitting of the titration curves always was less than 0.01 mL. Samples were kept in dark and deoxygenated by bubbling purified argon for *ca.* 10 min before the measurements and argon was also passed above the solutions during the titrations.

Protonation constants of the ligands were also determined in aqueous solutions by titrations with an HCl solution of known concentration (0.10 M) at an ionic strength of 0.10 M (KCl) and 25.0±0.1 ^{o}C. Under this condition pK_w is 13.76 ± 0.01 and the pH range of 11.5-2 was monitored.

Protonation constants of the ligands were determined with the computer program SUPERQUAD [31]. PSEQUAD [32] was utilized to establish the stoichiometry of the complexes and to calculate the stability constants (logβ_{MLH}). The calculations were always performed from data obtained prior to precipitation. The hydrolytic stability of these ligands was checked by a second titration with KOH following the back acidification of the initially

titrated sample. Constants calculated from the two consecutive titrations were found to be equal within ±0.05 log unites indicating that no decomposition occurred.

2.3. Spectrophotometric, spectrofluorimetric and ^{1}H NMR measurements

The Unicam Helios Alpha spectrophotometer was used to record the spectra in the region of 260-800 nm at 25 ^{o}C. Path length was 1 cm. UV-Vis spectrophotometric titrations were performed on the folate ligands in the pH range 2-13 and the concentration was 50 μM at an ionic strength of 0.10 M (KCl) in 60% (w/w) DMSO/H_2O. Protonation constants and the individual spectra of the species were calculated by the computer program PSEQUAD [32].

UV-visible spectrophotometric measurements on systems containing HSA at 10 μM and HEPES at 5 mM were performed by titration with 1 mM folic acid solution in order to obtain the difference spectra at pH 7.40. The HSA to ligand ratios were varied from 1:0.25 to 1:4. Control titration measurements were carried out under the same conditions with samples containing only the HEPES buffer without HSA.

Fluorescence spectra were recorded in a Hitachi-F4500 fluorimeter using 10 nm/10 nm slit width in 1 cm quartz cell at 25.0±0.1 ^{o}C. The binding constants were calculated with the computer program PSEQUAD [32] and by the modified Stern-Volmer linearization [33] for comparison (see SI for the sample preparation and calculations).

^{1}H NMR studies were carried out on a Brucker Ultrashield 500 Plus instrument. Folic acid or Fha were dissolved in a 60% (w/w) d_6-DMSO/D_2O (Sigma-Aldrich) mixture in 0.5 mM concentration and the Zn(II) to ligand ratios were 0:1 and 1:2. Chemical shifts are reported in ppm (δ) from tetramethylsilane as internal reference in d_6-DMSO.

2.4. Determination of the distribution coefficients

The distribution coefficients ($D_{o/w}$) of the folic acid and the folate derivatives were determined by the shake-flask method [34] in *n*-octanol/buffered aqueous solution at pH 5.30; 6.00 (MES); 7.40 (HEPES) and 8.00 (Tris) at 25.0±0.2 ^{o}C. All ligands were dissolved at 40 μM in the *n*-octanol pre-saturated aqueous solution of the buffer (0.01 M) containing KCl in 0.10 M. After shaking the aqueous solutions with *n*-octanol for 3 h, the mixtures were centrifuged at 4000 rpm for 15 min by a temperature controlled centrifuge (Sanyo). Two parallel experiments were performed for each sample. After the separation of the two phases,

pH values of the aqueous solution were controlled and confirmed to be equal within ±0.02 units to those of the starting buffered solution. UV-visible spectra of the ligands in the aqueous phase were compared with those of the starting aqueous solutions in the range 260–410 nm. $D_{o/w}$ was calculated as the mean of ($Abs_{original}$ / $Abs_{aqueous\ phase}$ − 1) obtained at the region of λ_{max} ±10 nm.

2.5. Membrane ultrafiltration

Samples were separated by ultrafiltration through 10 kDa membrane filters (Microcon YM-10 centrifugal filter unit, Millipore). All 0.50 mL samples contained 200 μM HSA and the folate ligands in 0.10 M HEPES buffer at pH 7.40 at 25.0±0.1 ^{o}C incubated for 2 h. The ligand concentrations were varied from 50 μM to 1.2 mM. After the separation by a temperature controlled centrifuge (Sanyo, 10000/s, 45-50 min), the low molecular mass (LMM) fractions were obtained. The filtrates were diluted to 5.00 mL and the concentrations of the non-bound ligand were determined by UV-Vis spectrophotometry. Mixtures of HSA and ligands at various ratios were used and the non-bound ligand fractions were separated by ultrafiltration from the HSA and HSA–ligand complexes in the high molecular mass fractions. The UV-Vis spectra of the LMM fractions were always compared with the reference spectra of the samples containing the ligand without protein in an analytical concentration equal to that in the ultrafiltered samples. Stoichiometries and conditional binding constants (logβ*) were then calculated with the computer program PSEQUAD [32] (see SI).

2.6. Electrospray ionization mass spectrometry (ESI-MS) measurements

ESI-MS spectra were recorded on a Waters Q-TOF Premier (Micromass MS Technologies, Manchester, UK) operating in positive ion mode. Samples were introduced into the ESI source by the syringe pump of the instrument. N_2 was used as nebulizer and cone gas, and the source temperature was set to 120 °C. The capillary voltage was set to 3.8 kV. Argon was employed as the collision gas and the collision energy was –25 eV. Samples contained the ligands in 0.20 mM concentration and $ZnCl_2$-to-ligand ratio was 0:1 or 1:2 in a non-buffered aqueous solution and pH 7.40 was set by addition of aqueous NH_3 and HNO_3.

3. Results

3.1. Proton dissociation processes

Determination of the proton dissociation constants of folic acid and its derivatives (shown in Scheme 1) has some difficulties in aqueous solutions by standard techniques such as pH-potentiometry due to their poor solubility in water, especially at the acidic pH range where the carboxylate groups are protonated. Furthermore, they can undergo oxidative photodegradation [35]. It was also found that folic acid has a tendency for self-association above 80 mM concentration [36]. Therefore, protonation could be followed by titrations with HCl till the appearance of precipitate (pH ~6) in aqueous solution and proton dissociation processes by titrations with KOH in a DMSO/H_2O solvent mixture when a wider pH range (pH 2–14) could be monitored. Aha, the simplest monohydroxamic acid and two prominent segments of folic acid, Pte and BzGlu were used as model compounds (shown in Scheme 1) for interpretation the data obtained for the folate ligands. Representative pH-potentiometric titration curves for folic acid and Fha in 60% (w/w) DMSO/H_2O are shown in Fig. 1 (for the model ligands see Fig. S1). Protonation constants determined by pH-potentiometry in the DMSO/H_2O mixture and in pure water are summarized in Tables 1 and 2, respectively. Data show that one p*K* could be determined for Aha, Pte, two for BzGlu, while three constants were calculated for the folate derivatives in the solvent mixture and only one or two in pure water.

Table 1

Table 2

Fig. 1

UV-Vis spectra of the folate ligands were recorded at different pH values in 60% (w/w) DMSO/H_2O, which revealed characteristic pH-dependent spectral changes in the wavelength range 260–435 nm. Similar behavior and spectra of the ligands were observed for all ligands studied, only the compounds containing phenyl moiety showed additional absorption in the wavelength range 260-280 nm. Decomposition of the ligands was not detected during the timescale of the measurements. It is noteworthy that the deprotonation of the hydroxamic and carboxylic acid functions was not accompanied by measurable spectral changes. Representative spectra for folic acid along with the calculated individual spectra for the ligand species (HL^{2-} and L^{3-}) are shown in Fig. 2 and for FProha in Fig. S2. The intense ligand bands at λ_{max} = 264 nm and 352/372 nm are assigned to the pteroyl fragments, while

the middle band (λ_{max} = 286 nm) belongs to the *p*-aminobenzoate moiety [37]. A bathochromic shift from λ_{max} = 352 nm to 372 nm, an increase in the absorbance of this absorption maximum (see Fig. S3), and a decrease at λ_{max} = 286 nm with development of a new shoulder band at λ_{max} = 264 nm could be observed due to the deprotonation at the pteroyl moiety. Isosbestic points at 271, 298 and 352 nm demonstrate that two species are involved in the equilibrium. Therefore, proton dissociation constants as microconstants for pteroyl moiety of the folate ligands (see Table 1) could be calculated based on the deconvolution of recorded UV-Vis spectra.

Fig. 2

Additionally, proton dissociation processes of Fha and those of folic acid for comparison were monitored by ^{1}H NMR titrations. It was found that chemical shifts (δ) of C*H*=N protons of the pteroyl moiety and C*H*=C-NH protons of the *p*-aminobenzoate residue exhibit reasonable sensitivity to the protonation state of both ligands (see Figs. 3 and S4). Upon deprotonation between pD ~7 and ~9 a significant upfield shift was obtained for the C*H*=N (s) protons and a minor downfield shift was observed for the C*H*=C-NH (d) protons. A downfield shift of δ of the C*H* (t) glutamate proton between pD ~10–12 was also observed that in the case of Fha.

Fig. 3

3.2. Characterization of the hydro-lipophilic properties of folate derivatives

The hydro-lipophilic character of the folate ligands was investigated via the determination of distribution coefficient ($D_{o/w}$) between *n*-octanol and buffered aqueous solutions in the pH range of 5.3–9.0. $D_{o/w}$ values for Fha, FProha, FPheha, folic acid, FPro and FPhe are depicted in Fig. 4 (see data in Table S1). The generally low solubility of the ligands in aqueous phase hindered the determination of the partition coefficient (*P*) referring to their neutral forms (H_3L^0); and predicted log*P* values are listed in Table S1.

Fig. 4

3.3. Interaction with human serum albumin

As a well-known drug carrier, HSA is able to bind mainly negatively charged, aromatic carboxylic acids (or large heterocyclic compounds) and to transfer them to the target tissues. HSA can solubilize poorly soluble drugs in the circulatory system via its ligand-

binding ability and it can also delay the metabolic clearance of therapeutic agents [38,39], that is why the interaction of the folates with HSA may have importance. At first, difference UV-Vis spectra were recorded at various protein-to-ligand ratios at physiological pH for samples containing the HSA and the simplest folate compound (folic acid), in order to obtain preliminary information whether the ligand binds to the protein. Difference spectra are depicted in Fig. 5, and measurable concentration-dependent ΔAbsorbance values were obtained due to the changes in the electronic structure of the ligand or the protein or both.

Fig. 5

Ultrafiltration–UV-Vis spectrophotometric measurements were carried out to determine the maximum number of ligands binding to HSA and the strength of the interaction in the case of folic acid, Fha, FPhe and Fheha. (Some typical UV-Vis spectra for the HSA–FPheha system are illustrated in Fig. S5.) Ratio of the spectrum of the LMM fraction to that of the reference sample gives the proportion of the number of moles of non-bound ligand to the total number of moles of the ligand. From these data pairs, the stoichiometries and conditional stability constants were calculated (see SI); and the results are listed in Table 3. The measured equilibrium concentrations of the bound ligands together with the values calculated by using the determined stability constants are presented in Fig. 6.

Fig. 6

Table 3

In addition, ultrafiltration –UV-Vis spectrophotometric measurements revealed that apoTf does not influence the binding of folic acid to HSA when blood serum conditions were used (see Fig. S6) according to the expectations based on literature data [20,21].

Fluorescence measurements were also performed on the binding properties of folic acid and its γ-hydroxamic and γ-carboxylic acid derivatives (Fha, FPhe, FPheha) towards HSA. This protein represents significant fluorescence as shown in the 3D spectra in Fig. 7.a due to the presence of the Phe, Tyr and Trp amino acids in its primary structure. It is well known that HSA contains a single Trp (at position 214) located in subdomain IIA, which can be selectively excited at λ_{EX} = 295 nm. The drug binding *site I* of HSA is situated nearby this Trp and ligand binding results in changes in its environment, which can be detected by spectrofluorimetry [39]. The fluorescence quenching of Trp-214 is clearly shown in the presence of folic acid in Figs. 7b, S7. Therefore, changes in fluorescence emission intensity of HSA were measured in the wavelength range 310–400 nm by the addition of the ligands at

various concentrations at λ_{EX} = 295 nm (see Fig.S8), and conditional binding constants (together with K_D values) were calculated and are listed in Table 3.

Fig. 7

Constants only for the first ligand binding step could be obtained due to the strong dissociation in the highly diluted solutions (μM range), which are *ca.* half order of magnitude higher than those obtained by the ultrafiltration–UV-Vis technique in a much higher concentration range. FPheha and Phe ligands have significant intrinsic emission at the excitation wavelength (see Fig. S9), which had to be considered in the calculations. Graphical solutions such as Stern-Volmer, Scatchard plots which are widely used in the literature [33,40], therefore, could not be not applied in the whole emission wavelength range, only where there is no ligand emission (*e.g.* λ_{EM} = 320 nm; see Fig. S8). Constants calculated by the modified Stern-Volmer linearization at λ_{EM} = 320 nm are also listed in Table 3 for comparison.

Displacement reactions with the anticoagulant drug warfarin, which is the mostly used and known site marker fluorescence probe for the binding *site I* of HSA [41], were performed. First of all interaction between HSA and warfarin was studied under the conditions (for the calculation see SI and Fig. S10), and log$K$* = 5.81(1) conditional binding constant was obtained, that is similar to published work [41]. The weak fluorescence emission of warfarin increased when it binds to HSA, while the displacement of the bound warfarin by the folate ligands is accompanied by a decrease of the intensity. (Ligands have no intrinsic emission in the wavelength range 330–400 nm at λ_{EX} = 310 nm.) Among the folate ligands only FPhe could compete significantly with warfarin (see Fig. S11)

3.4. Complex formation of folate derivatives with Zn(II)

The stability constants and stoichiometries of the complexes obtained upon pH-potentiometric titrations of Zn(II) with folic acid and its γ-hydroxamic and γ-carboxylic acid derivatives in the 60% (w/w) DMSO/H_2O solvent mixture are listed in Table 4. Calculations indicated the formation of *mono*-ligand species such as $[ZnL]^{-}$, $[ZnLH_{-1}]^{2-}$ and $[ZnLH_{-2}]^{3-}$ under the experimental conditions, and additionally [ZnLH] protonated complexes in the case of the hydroxamate derivatives. Stability constants for *bis*-ligand complexes could not be determined with certainty, therefore they were excluded from the accepted models. However, Roos *et al.* suggested the formation of *bis*-ligand complexes of folic acid [24]. Formation

constants for the complex $[ZnL]^-$ of folic acid obtained in aqueous solution by Kucharska *et al.* using different methods are somewhat lower than the our data [23,25].

In order to confirm the existence of these *mono*-ligand complexes ESI-MS was applied as data show in Table S2. The major signals in the ESI-MS spectra of the Zn(II)-folate systems arise from the metal-free ligands and the complexes with metal-to-ligand ratio 1:1. (The original number of the protons of the species in solution cannot be evaluated due to the limitation of this method.) Dimeric metal species or *bis*-ligand complexes could not be found by ESI-MS, while minimal dimerization of the metal-free ligands could be also observed owing to the stacking interactions *e.g.* between the pterine and the *p*-aminobenzoate rings [36].

Table 4

In order to obtain insight into the most probable binding modes of the folate derivatives, studies on complex formation of the model ligands, Pte, BzGlu and Aha with Zn(II) were also performed and the stability constants were determined (see Table 5). Negligible proton displacement from the ligand due to the Zn(II) coordination was observed during the titrations of Zn(II) and BzGlu containing systems, and the formation of a mixed hydroxide $[ZnL(OH)_2]^{2-}$ complex could be determined in the basic pH range, however, the coordination of the completely deprotonated ligand (L^{2-}) has no pH effect, hence its existence is rather uncertain. Pte was found to be a more efficient Zn(II) binder than BzGlu, and a similar stability data set was obtained as in the case of the γ-carboxylic acid derivatives.

Table 5

^{1}H NMR and ESI-MS fragmentation measurements were performed in order to obtain more information about the coordination modes in the Zn(II)-folic acid complexes. In the ^{1}H NMR spectra of Zn(II)-folic acid system (see Fig. S12.a) the signals of the metal-free and complexed ligand could not be distinguished due to the fast proton- and ligand-exchange processes, but some differences could be detected in the presence of Zn(II) compared to the spectra of the ligand alone. The coordination of Zn(II) results in alteration in the δ values of the C*H*=N and C*H*=C-NH protons monitored in the pH range of the formation of the *mono*-ligand $[ZnL]^-$ complex in comparison with the signals of the metal-free ligands.

ESI-MS collision-induced fragmentation (MS/MS) of the *mono*-ligand Zn(II) complex of folic acid (precursor ion: $[M+Zn-H]^+$ at 504 m/z; see Figs. 8 and S13 for some ionization patterns) results in the appearance of the signals of the typical fragments of the metal-free folic acid [42,43] formed by the neutral loss of the *p*-aminobenzamido-glumatyl and the glutamyl residues together with the most abundant product *p*-aminobenzoyl cation.

Additionally, Zn(II) containing species could be also identified at 375, 331, 357 m/z obtained by the loss of the glutamyl and the glutamine monoamide moieties.

Fig. 8

4. Discussion

4.1. Proton dissociation constants

In order to gain insight into the proton dissociation steps of the folate-γ-carboxylic and hydroxamic acids with the help of their p*K* values (see Table 1) those of the model ligands were analyzed first. Based on literature data it can be said that the p*K* of Aha is related to the -CONHOH → -CONHO$^-$ deprotonation process [44]. p*K* of Pte belongs undoubtedly to the pteroyl moiety and following the deprotonation the negative charge is mainly transferred to the enolic oxygen via the lactam-lactim tautomeric equilibrium [45] as Scheme 2 shows. BzGlu presents overlapping deprotonation of the two carboxylic acid moieties; but the proton dissociation starts most probably at the γ-COOH group, while the intermolecular hydrogen bridge between the α-COOH and the neighboring amide oxygen results in the deprotonation of the γ-carboxylic acid moiety taking place at higher pH [46].

Scheme 2

The three p*K* of the folate-γ-carboxylic acids show overlapping proton dissociation steps, but the order of γ-COOH, α-COOH and Pte moiety is the most probable based on the findings related to the model compounds above and literature data [46,47]. The deprotonation steps are much better separated in the case of the folate-γ-hydroxamic acids and the dissociation sequence of the α-COOH, the Pte and the hydroxamic acid moieties is the most likely.

p*K* values obtained in the DMSO/H_2O solvent mixture and in water show significant differences owing to the change in the medium permittivity (see Tables 1,2). Namely, the carboxylic and hydroxamic acid groups exhibit higher p*K* in the presence of DMSO, since the p*K* of anionic bases are increased as the dielectric permittivity of the solvent is decreased [48]. The p*K* of the pteroyl moiety, however, show merely a minor drift in the various media due to the strong hydrogen binding interaction between the enolate and the solvent molecules [47,49].

Effects of the various substituents on the p*K* values are also worth mentioning. Namely, the presence of the Phe and Pro residues results in lower p*K* of the hydroxamic and carboxylic acid functions (*cf.* p$K(H_3L)$, p$K(H_2L)$ of FPhe, FPro and those of folic acid; or p$K(H_3L)$, pK(HL) of FPheha, FProha and those of Fha in Table 1). It was also reported for simpler hydroxamic acids in our former work that phenyl and alkyl substituents on the carbon can decrease the p*K* value [44]. Additionally, the p*K* of the α-COOH groups in the case of the hydroxamate derivatives is significantly lower (~ 5) compared with that of the dicarboxylates (~ 6) most probably due to electron withdrawing effect of the hydroxamic acid moiety at the γ-position, as it was observed for glutamic acid and the corresponding hydroxamate (glutamyl-γ-hydroxamic acid) [50,51]. At the same time, the p*K* of the pteroyl moiety, which is far away from the substituents, does not show any considerably alteration in the case of the different folate ligands. The $pK_{(Pte\text{-}OH)}$ microconstants of the folate ligands obtained by UV-Vis titrations (see Table 1) were also found to be quite similar in all cases.

The ^{1}H NMR titrations revealed the similar changes of δ of C*H*=N (s) and C*H*=C-NH (d) protons, which are located quite close to the Pte ring, in the case of folic acid and Fha. This finding strongly support that the deprotonation of Fha also takes place at the pteroyl moiety in the range pD ~7 – 9, while the glutamate protons are found to be sensitive to the deprotonation of the hydroxamate residue.

4.2. Hydro-lipophilic properties

Based on the $D_{o/w}$ values of the folate ligands (see Fig. 4, Table S1) it can be concluded that (i) these compounds are strongly hydrophilic in the studied pH range (log$D_{o/w}$ always lower than –0.9); (ii) lipophilicity of the ligands is decreased (lower $D_{o/w}$ values) with increasing pH due to the deprotonation resulting in higher negative charges; (iii) compounds with Phe moieties represent higher lipophilicity, (iv) hydroxamate derivatization yields a somewhat increased lipophilic character due to the higher p*K* values.

4.3. Interaction with human serum albumin

Difference UV-Vis spectra (in Fig. 5) clearly show the interaction between HSA and the folic acid since the spectra of the ligand and the protein are not additive, while no appreciable interaction between folic acid and the other important serum protein, apoTf, was

found. The ultrafiltration studies reveal the formation of species with HSA:ligand composition of 1:1, 1:2 and 1:3, however, only the first binding step of the ligands has importance under realistic serum conditions, when the HSA to folate ratio is much less than 1 (see Table 3).

Significant quenching of emission of Trp-214 by the folate ligands could be detected. The conditional stability constants calculated by the modified Stern-Volmer approach at a chosen λ_{EM}, where the intrinsic emission of the ligands is negligible, or by the PSEQUAD program using the whole spectra (taking into account the emission of the ligands with Phe moiety) were found to be similar (see Table 3). Among the folate ligands FPhe could displace the site marker warfarin most efficiently. Concentration distribution curves for the HSA–warfarin–ligand systems calculated at various ligand concentrations (shown in Fig. S14) support this finding.

Constants obtained by the ultrafiltration and the fluorimetric studies show a moderate binding of the folate ligands to HSA. Fha and FPheha exhibit somewhat higher protein binding affinity compared with folic acid, while FPhe has prominent ability to bind to the HSA. The *site I* of HSA is suggested to be their primary binding site.

4.4. Zn(II) complexes of the folates and the model compounds

Concentration distribution curves were calculated based on the stability constants collected in Table 4, and are plotted as a function of pH in order to compare the pH range and the extent of the complex formation in the Zn(II)–folic acid and –Fha systems (see Fig. 9). Analysis of these curves shows that the coordination process starts with Fha at somewhat lower pH, with the formation of [ZnLH] complex, as compared with folic acid and a higher molar fraction of $[ZnL]^-$ when L=Fha. $[ZnLH_{-1}]^{2-}$ and $[ZnLH_{-2}]^{3-}$ species predominate above pH ~9, which should be regarded as mixed hydroxido complexes $[ZnL(OH)]^{2-}$ and $[ZnL(OH)_2]^{3-}$ resulting from the deprotonation of coordinated water molecules. FPro and FPhe ligands demonstrate similar stability constants and behavior as folic acid, while concentration distribution curves calculated for the hydroxamate derivatives revealed that FProha is a slightly weaker binder of Zn(II) compared to Fha and FPheha (not shown here), most probably because of the more rigid character of the Pro moiety.

Fig. 9

All compounds studied as multidentate ligands provide different coordination possibilities: besides binding via the pteridinic moieties the folate-γ-carboxylic acids may

coordinate via the glutamate, and the folate-γ-hydroxamic acids via the hydroxamate oxygens. Literature data on the binding modes of complexes formed between folic acid and divalent transition metal ions show that the ligand can coordinate via the pteridinic ($O_{(4\text{-}OH)}$,$N_{(5)}$) or mainly via the ($O_{(4\text{-}OH)}$,$N_{(5)}$,$N_{(10)}$) donor sets [24,52-54] as it is depicted in Scheme 3, but data are rather contradictory for coordination via glutamate carboxylates [55,56].

Scheme 3

Since the interaction between BzGlu and Zn(II) was found to be almost negligible (See Table 5), coordination of folic acid and its γ-carboxylate derivatives via the pteridinic moiety is the most probable, and the contribution of the glutamate carboxylates is insignificant. The derived constant of Pte for the stability of the metal chelate compared with the proton complex (see the last row in Table 5) is somewhat lower as in the case of folic acid. Most probably the formation of the fused chelate rings (($O_{(4\text{-}OH)}$,$N_{(5)}$,$N_{(10)}$) coordination) in the Zn(II)-folate-γ-carboxylate complexes results in higher stability compared with the bidentate (O,N) binding mode of Pte.

^{1}H NMR studies on the Zn(II)-folic acid system could confirm the pH range of the formation of the mono-ligand Zn(II) species, which is expected based on the speciation model and the higher δ values in the presence of Zn(II) compared with those of the metal-free ligand at the same pH values are assumed due to the formation of the fused chelate rings, ($O_{(4\text{-}OH)}$,$N_{(5)}$,$N_{(10)}$) binding. The ESI-MS collision-induced fragmentation in the same system showed that the Zn(II)-pteridinyl coordination mode is preserved during the experiment.

In the case of the folate-hydroxamate derivatives coordination to Zn(II) via the hydroxamate oxygen donor atoms is assumed (see Scheme 3) since their inhibitory activity against a series of MMPs [10] is based on their ability to bind to the Zn(II) centers via the bidentate (O,O) set in contrast with folic acid, which is not active at all [10]. On the other hand, the pH-dependent conditional stability constants of the [ZnL] complex of folic acid and the model hydroxamic acid, Aha are quite comparable at neutral pH as Fig. 10 represents, and the (O,O) coordination mode becomes more favorable than the ($O_{(4\text{-}OH)}$,$N_{(5)}$,$N_{(10)}$) only at the basic pH range. Thus, the folic acid type coordination of the folate-hydroxamate conjugates at the physiological pH range cannot be excluded; and ^{1}H NMR results showed quite similar changes of the δ values of the protons on the pteridinic moiety (see S11.b) as it was detected for folic acid. This finding suggests that these ligands may coordinate not merely via hydroxamate oxygens but also through the other donor atoms of the molecules to form linkage isomers.

Fig. 10

4. Conclusions

Interaction of folic acid and various MMP inhibitor γ-hydroxamic acid derivatives with HSA in aqueous solution and with Zn(II) in a DMSO/water mixture was studied in order to clarify the stoichiometry and stability of the species formed. Some model ligands such as the analogue folate-γ-carboxylic acid derivatives and prominent segment molecules (Aha, BnGlu, Pte) were involved for comparison. The folate ligands show highly hydrophilic character at physiological pH range, and the introduction of the hydroxamate and Phe moieties results in an increase in the lipophilicity. Moderate binding of the compounds to HSA was found, and folate-γ-Phe exhibits the highest binding constant. This behavior may have effect on the transport processes of these ligands in the serum, thus on the rate of the metabolic clearance.

Coordination of folic acid via the pteridine moiety was found in the Zn(II)-*mono*-ligand complexes and the tridentate ($O_{(4\text{-}OH)}$,$N_{(5)}$,$N_{(10)}$) binding mode is suggested. The Zn(II) complexes of the different folate-hydroxamate derivatives represent similar binding strength and the formation of linkage isomers (coordination via the pteridine or the hydroxamate group) is possible; however the bidentate hydroxamate-type binding to the active Zn(II) center is the most probable when these ligands act as inhibitors of the MMPs. It is noteworthy that the prominent inhibitory activity of the ligand FPheha [10] seems to be more determined by the lipophilic character, resulting in stronger hydrophobic interactions with the enzymes, than by the stability of the Zn(II)-chelate.

Supplementary data

Mathematical background of the calculation of the binding constants, figures for some titration curves, pH-dependent UV-Vis, ^{1}H NMR spectra and chemical shifts, fluorescence spectra, ESI-MS results and concentration distribution curves are shown.

5. Abbreviations

Aha	acetohydroxamic acid

apoTf	apotransferrin
BzGlu	benzoylglutamic acid
CHES	*N*-cyclohexyl-2-aminoethanesulfonic acid
CT	charge transfer
$D_{o/w}$	distribution coefficient
DTPA	diethylenetriaminepentaacetic acid
ε	molar absorptivity
ESI-MS	electrospray ionization mass spectrometry
Fha	folate-γ-hydroxamic acid
FPhe	folate-γ-phenylalanine
FPheha	folate-γ-phenylalanine hydroxamic acid
FPro	folate-γ-proline
FProha	folate-γ-proline hydroxamic acid
HSA	human serum albumin
HEPES	4-(2-hydroxyethyl)-1-piperazineethanesulfonic acid
λ_{EM}	fluorescence emission wavelength
λ_{EX}	fluorescence excitation wavelength
LMM	low molecular mass
MES	2-(*N*-morpholino)ethanesulfonic acid
MMPs	matrix metalloproteinases
P	partition coefficient
Pte	pterine

Acknowledgments

This work has been supported by the Hungarian Research Foundation OTKA K77833, OTKA-NKTH CK77586, TAMOP 4.2.1./B-09/1/KONV-2010-0007 and the Portuguese Science Foundation (FCT). É.A. Enyedy gratefully acknowledges the financial support of J. Bolyai research fellowship. We thank Ms. Katalin Tóth-Szűcs for the pH-potentiometric and Dr. Zoltán Kele for the ESI-MS measurements.

References

[1] A.R. Hilgenbrink, P.S. Low, J. Pharm. Sci. 94 (2005) 2135-2146.

[2] C.P. Leamon, J.A. Reddy, Advanced Drug Delivery Reviews 56 (2004) 1127-1141

[3] C.P. Leamon, P.S. Low, Drug Discovery Today 6 (2001) 44-51.

[4] B.A. Siegel, F. Dehdashti, D.G. Mutch, D.A. Podoloff, R. Wendt, G.P. Sutton, R.W. Burt, P.R. Ellis, C.J. Mathias, M.A. Green, D.M. Gershenson, J. Nucl. Med. 44 (2003) 700-707.

[5] S. Wang, R.J. Lee, C.J. Mathias, M.A. Green, P.S. Low, Bioconjugate. Chem. 7 (1996) 56-62.

[6] R. Rossin, D. Pan, K. Qi, J.L.Turner, X. Sun, K.L. Wooley, M.J. Welch, J. Nucl. Med. 46 (2005) 1210-1218.

[7] C. Müller, J.A. Reddy, C.P. Leamon, R. Schibli, Mol. Pharm. 7 (2010) 597-604.

[8] J. Walling, Invest. New Drugs 24 (2006) 37-77.

[9] D. Exinger, F. Exinger, B. Mennecier, J.M. Limacher, P. Dufour, J.E. Kurtz, Cancer Therapy 1 (2003) 315-322.

[10] M.A. Santos, E.A. Enyedy, E. Nuti, A. Rossello, N.I. Krupenko, S.A. Krupenko, Bioorg. Med. Chem. 15 (2007) 1266-1274.

[11] Roy R, Yang J, Moses MA. J Clin Oncol. 27 (2009) 5287-5297.

[12] E.I. Deryugina, J.P. Quigley, Cancer and Metastasis Reviews 25 (2006) 9-34.

[13] J.F. Fisher, S. Mobashery, Cancer and Metastasis Reviews 25 (2006) 115-136.

[14] S.M. Marques, E.A. Enyedy, C.T. Supuran, N.I. Krupenko, S.A. Krupenko, M.A. Santos, Bioorg. Med. Chem. 18 (2010) 5081-5089.

[15] M. Tegoni, F. Dallavalle, M.A. Santos, J. Inorg. Biochem. 98 (2004) 209-218.

[16] C.T. Supuran, A. Casini, A. Scozzafava, Med. Res. Rev. 23 (2003) 535-558.

[17] J.H. Hooijberg, N.A. de Vries, G.J.L. Kaspers, R. Pieters, G. Jansen, G.J. Peters, Cancer Chemother. Pharmacol. 58 (2006) 1-12.

[18] T. Markkaren, R.L. Pajula, P. Himanen, S. Virtanen, J. Clin. Path. 26 (1973) 486-493.

[19] U. Christensen, J. Holm, S.I. Hansen, Biosci. Rep. 26 (2006) 291-299.

[20] H.A. Soliman, H. Olesen, Scand. J. Clin. Lab. Invest. 36 (1976) 299-304.

[21] J. Holm, S.I. Hansen, J. Lyngbye, Biochim. Biophys. Acta 629 (1980) 539-545.

[22] D.B. Milne, W.K. Canfield, J.R. Mahalko, H.H. Sandstead, Am. J. Clin. Nutr. 39 (1984) 535-539.

[23] J. Maslowska, U. Kucharska, Polish J. Chem. 69 (1995) 1463-1473.

[24] J.T.H. Roos, D.R. Williams, J. Inorg. Nucl. Chem. 39 (1977) 367-369.
[25] U. Kucharska, Talanta 44 (1997) 85-96.
[26] SCQuery, The IUPAC Stability Constants Database, Academic Software (Version 5.5), Royal Society of Chemistry, 1993-2005.
[27] G. Gran, Acta Chem. Scand. 4 (1950) 559-577.
[28] N. D. Chasteen, J.K. Grady, C. E. Holloway, Inorg. Chem. 25 (1986) 2754-2760.
[29] G. H. Beaven, S. H. Chen, A. d'Albisi, W.B. Gratzer, Eur. J. Biochem. 41 (1974) 539-546.
[30] H.M. Irving, M.G. Miles, L.D. Pettit, Anal. Chim. Acta 38 (1967) 475-488.
[31] A. Sabatini, A. Vacca, P. Gans, Talanta 21 (1974) 53-77.
[32] L. Zékány, I. Nagypál, in: Computational Methods for the Determination of Stability Constants (Ed.: D. L. Leggett), Plenum Press, New York, 1985, pp. 291-353.
[33] M.R. Eftink, C.A. Ghiron, Anal. Biochem. 114 (1981) 199-227.
[34] A. Avdeef, B. Testa, CMLS, Cell. Mol. Life Sci. 59 (2002) 1681-1689.
[35] E.A. Mironov, V.S. Nabokov, Khimiko-Farmatsevticheskii Zhurnal 10 (1976) 136-140.
[36] M. Poe, J. Biol. Chem. 248 (1973) 7025-7032.
[37] J.S. Erickson, C.K. Mathews, J. Biol. Chem. 247 (1972) 5661-5667.
[38] M. Fasano, S. Curry, E. Terreno, M. Galliano, G. Fanali, P. Narciso, S. Notari, P. Ascenzi, IUBMB Life 57 (2005) 787-796.
[39] K.J.Fehske, W.E. Muller, U. Wollert, Mol. Pharmacol. 16 (1979) 778-789.
[40] J.R. Lakowicz, Principles of fluorescence spectroscopy, 3rd. ed., Springer Science, New York, 2006.
[41] D.E. Epps, T.J. Raub, F.J. Kezdy, Anal. Biochem. 227 (1995) 342-350.
[42] J.D.M. Patring, J.A. Jastrebova, J. Chromatography A 1143 (2007) 72-82.
[43] C.E. Hignite, D.L. Azarnoff, Biomed. Mass Spect. 5 (1978) 161-163.
[44] E. Farkas, E.A. Enyedy, H. Csoka, J. Inorg. Biochem. 79 (2000) 205-211.
[45] D.J. Brown, S.F. Mason, J. Chem. Soc. 1956, 3443-3453.
[46] Z. Szakács, PhD thesis (2005)
[47] Z. Szakács, B. Noszál, Electrophoresis 27 (2006) 3399-3409.
[48] N.A. Izmailov, Electrochemistry of solutions, 2nd ed., Khimia, Moscow, 1966
[49] R.G. Bates, J. Electroanal. Chem. 29 (1971) 1-19.
[50] E. Farkas, K. Megyeri, L. Somsák, L. Kovács, J. Inorg. Biohem. 70 (1998) 41-47.
[51] T. Kiss, I. Sóvágó, I. Tóth, A. Lakatos, R. Bertani, A. Tapparo, G. Bombi, R.B. Martin, Chem. Soc. Dalton Trans. 1997, 1967-1972.

[52] A. Albert, Biochem. J. 54 (1953) 646-654.
[53] A. Thomas, E. Wolcan, M.R. Feliz, A.L. Capparelli, Transition Met. Chem. 22 (1997) 541-544.
[54] D.H. Lee, N.N. Murthy, Y. Lin, N.S. Nasir, K.D. Karlin, Inorg. Chem. 36 (1997) 6328-6334.
[55] M.G. Abd El-Wahed , M.S. Refat, S.M. El-Megharbel, Spectrochimica Acta Part A 70 (2008) 916–922.
[56] E. Hamed, M.S. Attia, K. Bassiouny, Bioinorg. Chem. Appl. (2009) 979680.

Figures/Scheme Legends

Scheme 1 Folate ligands used in this study: **Fha** = folate-γ-hydroxamic acid; **Folic acid**; **FProha** = folate-γ-proline hydroxamic acid; **FPro** = folate-γ-proline; **FPheha** = folate-γ-phenylalanine hydroxamic acid and **FPhe** = folate-γ-phenylalanine; and formulae of the model ligands: **Aha** = acetohydroxamic acid; **BzGlu** = benzoylglutamic acid; **Pte** = pterine.

Scheme 2 Lactam-lactim tautomers of the pteroyl moiety.

Scheme 3 Proposed binding modes of the coordination of the pteridinic (a) and the hydroxamate (b) moieties.

Fig. 1 Representative pH-potentiometric titration curves for folic acid and Fha {c_{ligand} = 2 mM; t = 25 ˚C, I = 0.10 M (KCl) in 60% (w/w) DMSO/H_2O}. *Negative base equivalent values mean acid excess.*

Fig. 2 UV-Vis absorption spectra of folic acid recorded at different pH values {c_{ligand} = 54 μM; t = 25 ˚C, I = 0.10 M (KCl) in 60% (w/w) DMSO/H_2O}. *Inset shows the calculated individual absorbance spectra of HL^{2-} and L^{3-} species of folic acid.*

Fig. 3 pD-dependent chemical shifts (ppm) for C*H*=N (s) and C*H*=C-NH (d) protons of folic acid (●) and Fha (×) measured by ^{1}H NMR titration {c_{ligand} = 2 mM; 60% (w/w) DMSO/D_2O}.

Fig. 4 Octanol/water distribution coefficient ($D_{o/w}$) of folic acid and some folate derivatives measured at different pH {c_{ligand} = 40 μM; t = 25 ˚C, I = 0.10 M (KCl)}. (Data with $D_{o/w}$ = 0 have the meaning that the UV spectra of the starting and the separated aqueous solutions did not show measurable differences (ΔAbs <0.005 at λ_{max})).

Fig. 5 UV-Vis absorption difference spectra of folic acid – HSA system in addition of folic acid recorded at pH = 7.40 (5 mM HEPES) {c_{HSA} = 10 μM; HSA to folic acid ratio = 1:x where x = 0.5 (a), x = 1 (b), x = 2 (c), x = 4 (d), t = 25.0 ˚C}. ΔAbsorbance = Abs(HSA-folic acid) – (Abs(HSA) – Abs(folic acid).

Fig. 6 Ratio of the equilibrium concentrations of the bound folate ligand to *c*(HSA) *vs.* *c*(ligand)/*c*(HSA) for folic acid (♦), FPhe (▲), Fha (x) and FPheha (○) at pH = 7.40 (0.10 M HEPES). Calculated values on the basis of the determined associative conditional binding constants are also presented (solid lines: folic acid (a), FPhe (b), Fha (c) or FPheha (d)).

Fig. 7 3D fluorescence spectra of HSA (a) and HSA – folic acid (1:10) system (b) {c_{HSA} = 7.5 μM; t = 25 ˚C; pH = 7.40 (0.4 mM HEPES); PTM = 700 V; Slits: 10/10 nm}.

Fig. 8 ESI-MS collision-induced fragmentation spectrum (MS/MS) of the parent peak of $[M+Zn-H]^+$ at m/z 504 recorded in Zn(II) – folic acid ($c_{folic\ acid}$ = 0.20 mM; M : L = 1:1; pH = 7.50)

Fig. 9 Concentration distribution curves for Zn(II)-folic acid (solid lines) and Zn(II)-Fha (dashed lines) systems {c_{ligand} = 1 mM; metal-to-ligand ratio 1:2; t = 25.0˚C, I = 0.10 M (KCl) in 60% (w/w) DMSO/H_2O}.

Fig. 10 The pH dependence of conditional stability constants log$K$(ZnL)* calculated for [ZnL] *mono* complexes of Zn(II) formed with folic acid (■) and the model ligand Aha (□) as representatives for the (O,N,NH) pteridinic and (O,O) hydroxamate coordination modes, respectively. (log$K$(ZnL)* = log(β(ZnL)/α_H); $\alpha_H = 1 + \beta(HL)\times[H^+]$)

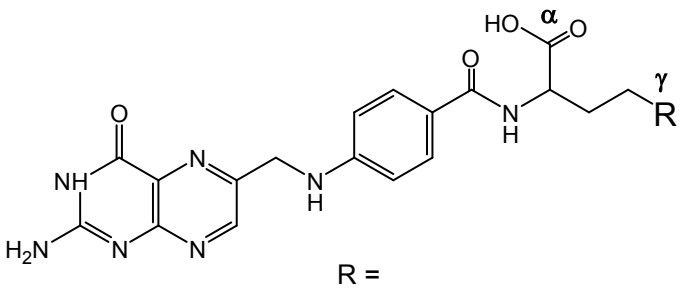

R =

Fha -CONHOH **Folic acid** -COOH

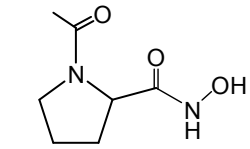

FProha

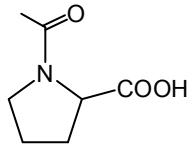

FPro

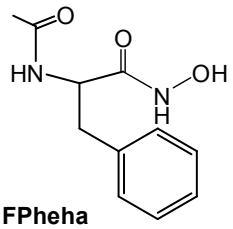

FPheha

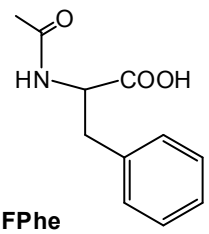

FPhe

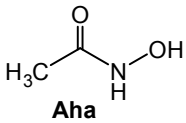

Aha

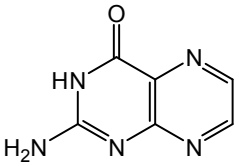

Pte

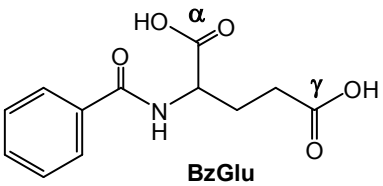

BzGlu

Scheme 1

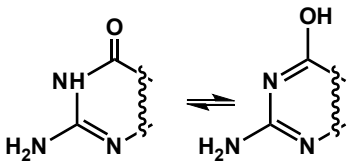

Scheme 2

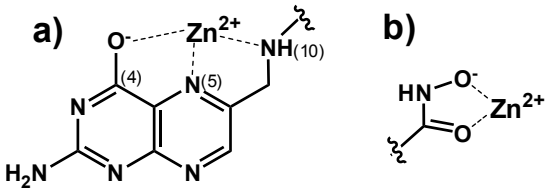

Scheme 3

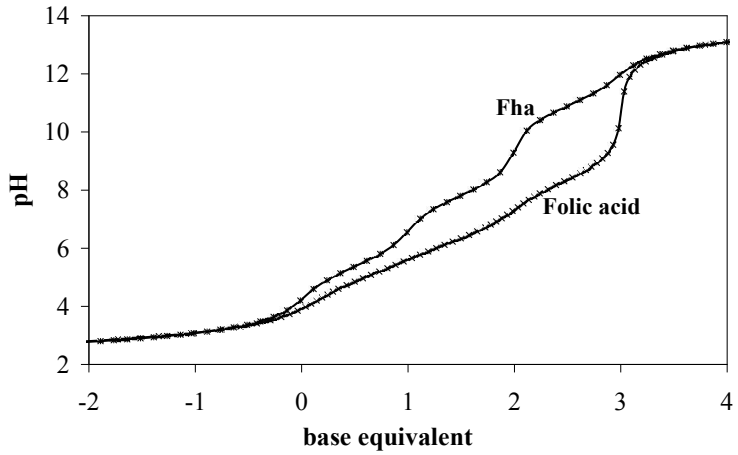

Fig. 1

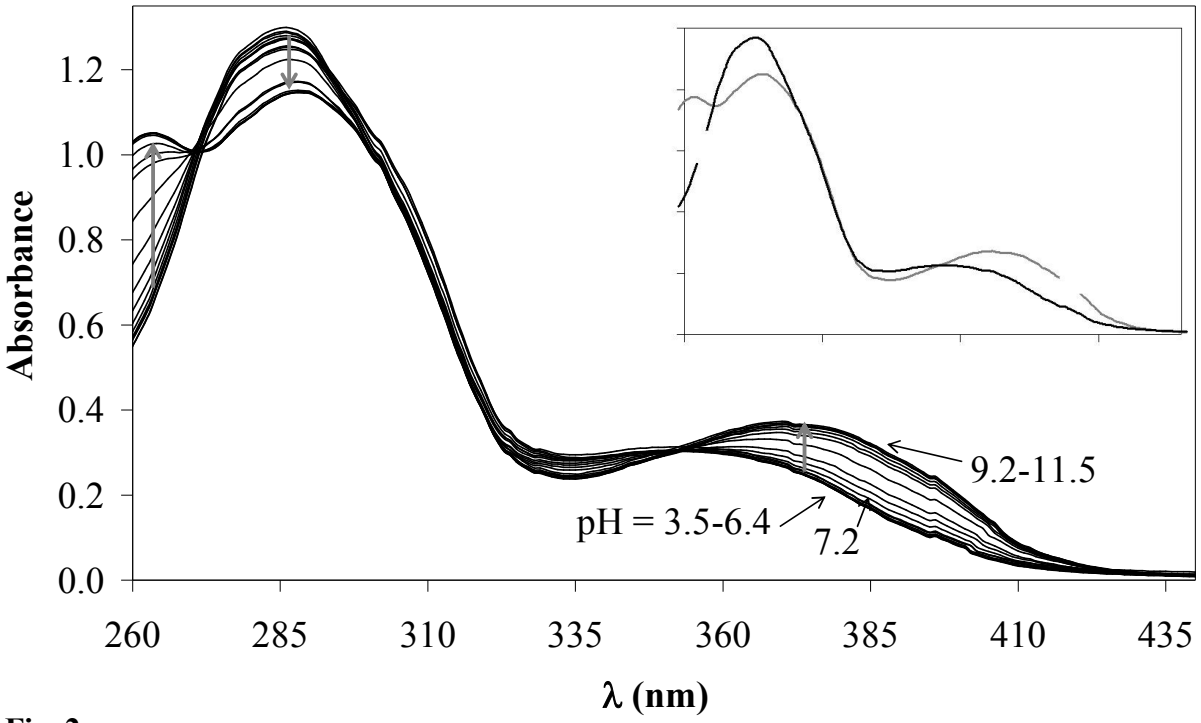
Absorbance
1.2
1.0
0.8
0.6
0.4
0.2
0.0
260
285
310
335
360
385
410
435
λ (nm)
9.2-11.5
pH = 3.5-6.4
7.2

Fig. 2

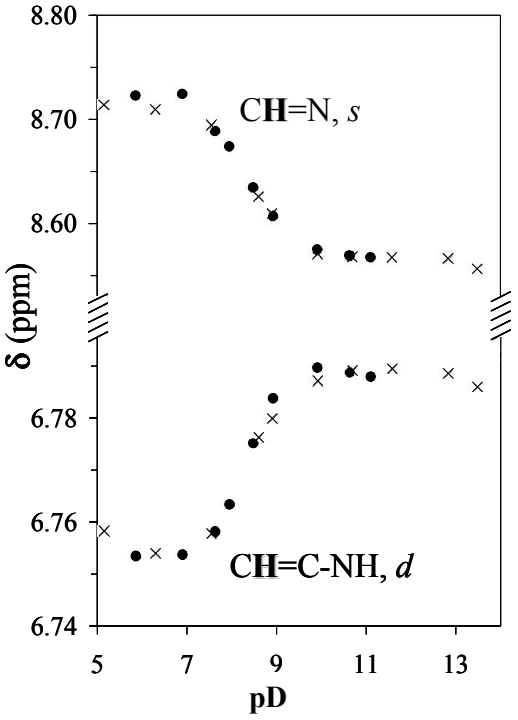

Fig. 3

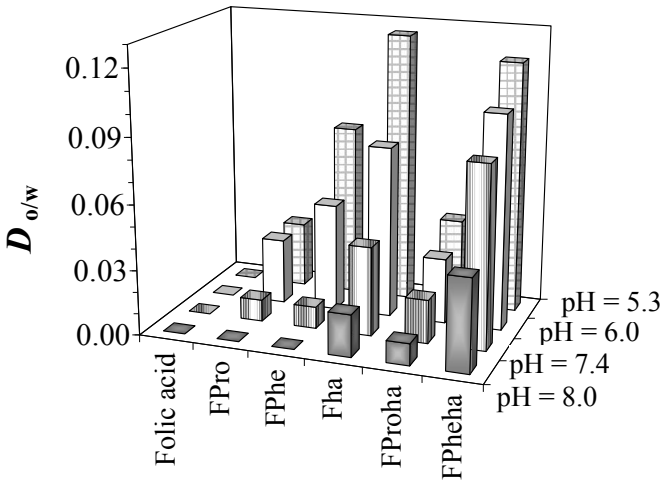

Fig. 4

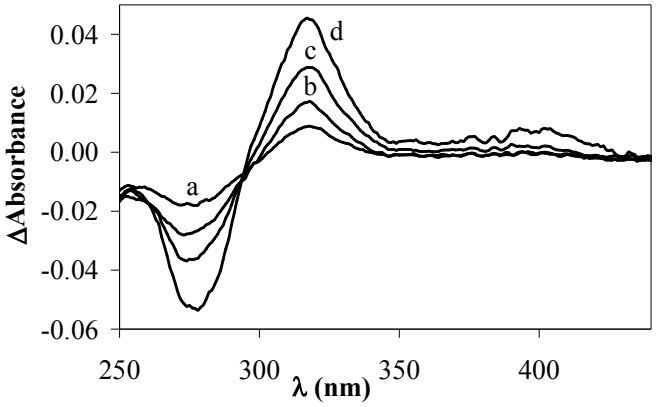

Fig. 5

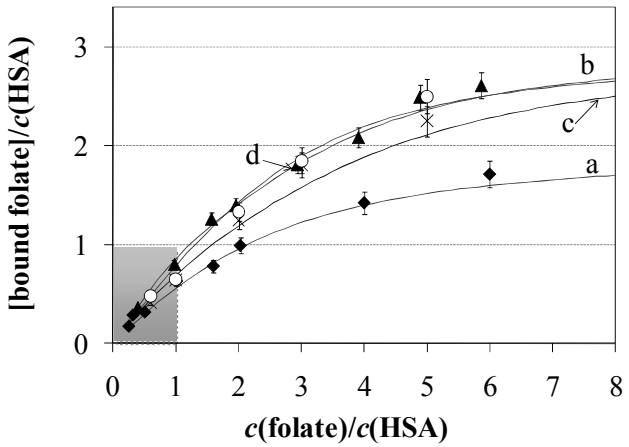

Fig. 6

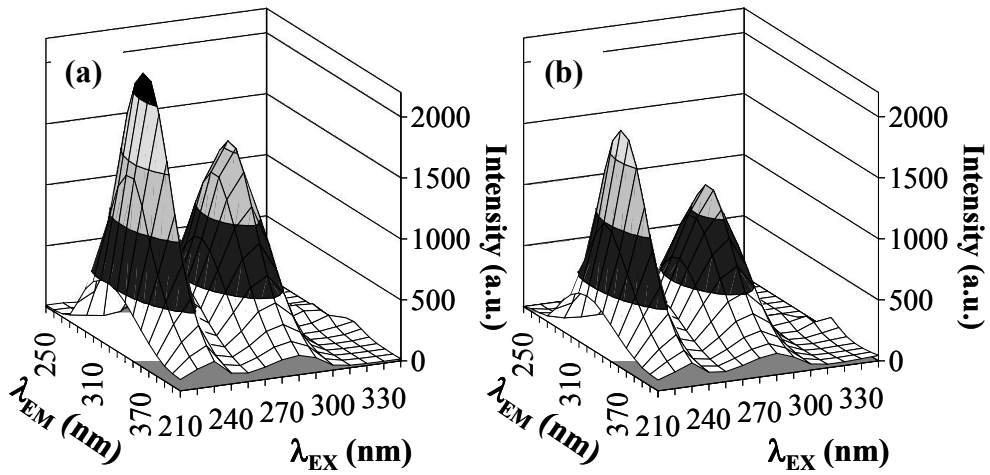
(a)
(b)
2000
1500
1000
500
0
Intensity (a.u.)
250
310
370
λEM (nm)
210 240 270 300 330
λEX (nm)

Fig. 7

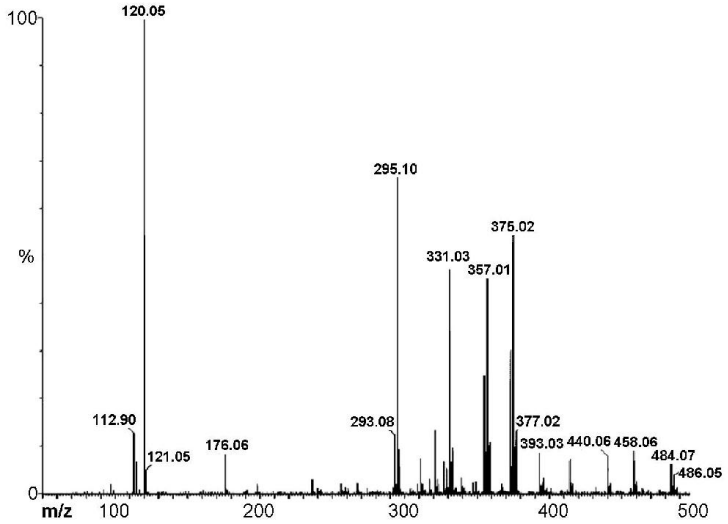
100
%
0
120.05
295.10
375.02
331.03
357.01
112.90
121.05
176.06
293.08
377.02
393.03
440.06
458.06
484.07
486.05
m/z
100
200
300
400
500

Fig. 8

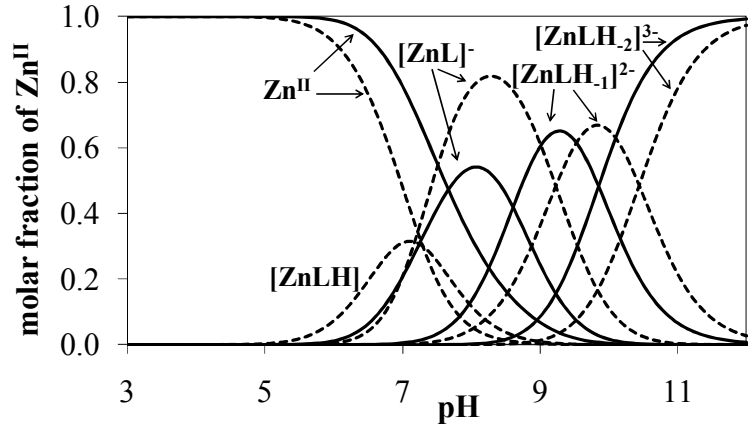
molar fraction of Zn^II
1.0
0.8
0.6
0.4
0.2
0.0
3
5
7
9
11
pH
Zn^II
[ZnL]-
[ZnLH]
[ZnLH-2]3-
[ZnLH-1]2-

Fig. 9

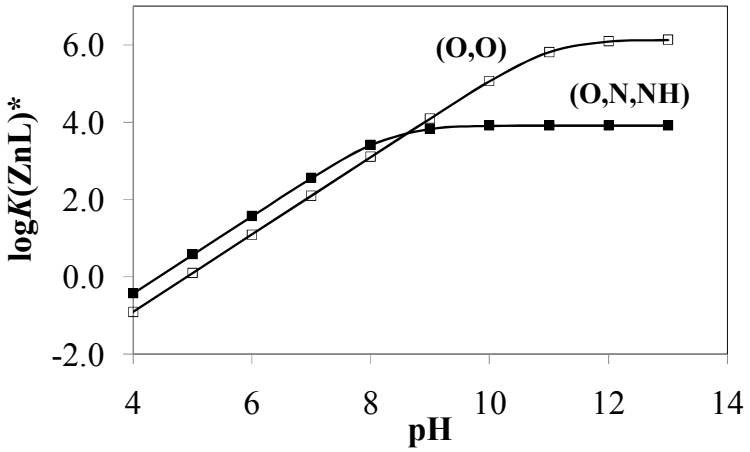
logK(ZnL)*
6.0
4.0
2.0
0.0
-2.0
4
6
8
10
12
14
pH
(O,O)
(O,N,NH)

Fig. 10

Table 1

Protonation and dissociation constants ($\log\beta(H_iL)$; pK_i) of the folate-γ-hydroxamic and dicarboxylic acid derivatives and some model compounds [60% (w/w) DMSO/water; t = 25°C; I = 0.10 M (KCl)][a]

	$\log\beta$ (HL)	$\log\beta(H_2L)$	$\log\beta(H_3L)$	$pK(H_3L)$	$pK(H_2L)$	pK(HL)	$pK_{(Pte\text{-}OH)}$[d]
Folic acid[b]	8.34(2)	14.66(3)	19.52(4)	4.86	6.32	8.34	8.21(1)
FPro	8.38(4)	14.41(5)	18.98(7)	4.57	6.03	8.38	8.02(1)
FPhe	8.20(4)	14.14(5)	18.69(8)	4.55	5.94	8.20	8.07(1)
Fha	10.91(9)	18.73(9)	24.1(1)	5.4	7.82	10.91	7.98(2)
FProha	10.54(8)	18.50(5)	23.5(1)[c]	~5[c]	7.96	10.54	7.92(1)
FPheha	10.41(5)	18.28(7)	23.28(9)	5.00	7.87	10.41	7.85(1)
Aha	11.03(1)	–	–	–	–	11.03[e]	–
BzGlu	6.35(1)	11.20(2)	–	–	4.85	6.35	–
Pte	8.95(2)	–	–	–	–	8.87[f]	–

[a] Standard deviations (SD) in parenthesis

[b] Literature data under similar conditions {62.1% (w/w) DMSO/H_2O; t = 25°C; I =0.15 M, (KCl)}: pK_1 = 4.91; pK_2 = 6.41; pK_3 = 8.10 [46].

[c] Not well determined due to the low solubility at lower pH range.

[d] Determined by UV-Vis spectrophotometric titrations at pH > 7.5.

[e] pK_a of the hydroxamic acid moiety.

[f] pK_a of the pteroyl moiety.

Table 2

Protonation and dissociation constants ($\log\beta(H_iL)$; pK_i) of the folate-γ-hydroxamic and dicarboxylic acid derivatives in aqueous solution [t = 25°C; I = 0.10 M (KCl)][a]

	$\log\beta$ (HL)	$\log\beta$ (H_2L)	pK(H_2L)	pK(HL)
Folic acid	8.04(2)	12.96(7)	4.92	8.04[b]
FPro	7.98(3)	–	–	7.98
FPhe	8.07(6)	–	–	8.07
Fha	9.19(2)	16.73(4)	7.54	9.19
FProha	9.06(2)	16.62(4)	7.56	9.06
FPheha	9.12(1)	16.42(3)	7.30	9.12
Aha	9.27[c]	–	–	9.27[d]

[a] Standard deviations (SD) in parenthesis.
[b] pK (PteOH) = 8.06(2) determined by UV-Vis titrations.
[c] Data taken from Ref. [44], {I = 0.20 M (KCl)}.
[d] pK of the hydroxamic acid moiety.

Table 3

Conditional binding constants ($\log\beta'$) of the HSA – folate complexes determined by ultrafiltration and spectrofluorimetry[a]

	Folic acid	Fha	FPhe	FPheha
ultrafiltration				
$\log\beta^*_1$ (HSA-L)[b]	3.92(4)	4.31(5)	5.04(5)	4.4(1)
$\log\beta^*_2$(HSA-L_2)[b]	7.29(6)	7.7(1)	8.6(1)	8.3(1)
$\log\beta^*_3$(HSA-L_3)[b]		~11	12.0(1)	11.7(2)
$\log K^*_1$[b]	3.92	4.31	5.04	4.4
$\log K^*_2$[b]	3.37	3.4	3.6	3.9
$\log K^*_3$[b]		3.3	3.4	3.4
spectrofluorimetry				
$\log K^*$[c]	4.67(5)	4.7(1)	5.74(4)	5.04(3)
K_D[c]	21.4 μM	17.8 μM	1.8 μM	9.1 μM
$\log K^*_{S.V.}$[d]	4.6(1)	4.5(1)	5.4(1)	5.0(1)
K_D[d]	56 μM	36 μM	5 μM	10 μM

[a] Standard deviations (SD) in parenthesis.
[b] t = 25°C; 0.10 M HEPES; c_{HSA} = 0.200 mM.
[c] t = 25°C; 0.4 m M HEPES; c_{HSA} = 0.8 μM; $K_D = 1/K^*$ {λ_{EX} = 295 nm; λ_{EM} = 310–400 nm}.
[d] Calculated by the modified Stern–Volmer linearization of $I_0/(I_0–I)$ vs. $1/c_{ligand}$ [33]; $K_D = 1/K^*$ (λ_{EX} = 295 nm; λ_{EM} = 320 nm).

Table 4

Overall stability constants of Zn(II) complexes of folate-γ-hydroxamic and dicarboxylic acid derivatives [60% (w/w) DMSO/water; t = 25°C; I = 0.10 M (KCl)][a]

	Folic acid	**FPro**	**FPhe**	**Fha**	**FProha**	**FPheha**
logβ ([ZnLH])	–	–	–	14.74(13)	14.03(15)	14.35(9)
logβ ([ZnL]$^{-}$)	3.92(8)	3.98(9)	4.01(12)	7.56(5)	6.98(4)	6.98(4)
logβ ([ZnLH$_{-1}$]$^{2-}$)	–4.69(8)	–3.78(5)	–3.55(7)	–1.67(7)	–1.80(5)	–1.58(5)
logβ ([ZnLH$_{-2}$]$^{3-}$)	–14.54(9)	–11.96(4)	–12.36(9)	–12.11(10)	–13.49(9)	–12.76(9)
fitting parameter (mL)	2.91×10^{-3}	1.37×10^{-3}	3.71×10^{-3}	4.15×10^{-3}	2.75×10^{-3}	2.11×10^{-3}

[a] Standard deviations (SD) in parenthesis.

Table 5

Overall stability constants of Zn(II) complexes of model compounds (Aha, Pte and BnGlu) [60% (w/w) DMSO/water; t = 25°C; I = 0.10 M (KCl)][a]

	Aha	**Pte**	**BnGlu**
$\log\beta(ZnL)$[b]	6.13(2)	3.9(1)	–
$\log\beta(ZnLH_{-1})$[b]	–2.11(4)	–3.54(4)	–
$\log\beta(ZnLH_{-2})$[b]	–13.40(2)	–12.71(5)	–13.45(4)
$\log\beta(ZnL_2)$[b]	11.75(5)	–	–
$\log\beta(ZnL_3)$[b]	15.30(5)	–	–
fitting parameter (mL)	2.95×10^{-3}	7.49×10^{-3}	7.23×10^{-3}
$\log K(ZnL) - pK$[c]	–4.90	–5.05	–

[a] Standard deviations (SD) in parenthesis.
[b] Charges are omitted for simplicity.
[c] For folic acid: $\log K(ZnL) - pK_3 = -4.42$.